

Title	Correlations between alpha particles and ejectiles in the 208 MeV ^{14}N on ^{93}Nb reaction at three different ejectile angles
Author(s)	Fukuda, T.; Ishihara, M.; Tanaka, M.; Ogata, H.; Miura, I.; Inoue, M.; Shimoda, T.; Katori, K.; Nakayama, S.
Citation	Physical Review C. 27(5) P.2029-P.2036
Issue Date	1983-05
Text Version	publisher
URL	http://hdl.handle.net/11094/23138
DOI	10.1103/PhysRevC.27.2029
rights	Fukuda, T. , Ishihara, M. , Tanaka, M. , Ogata, H. , Miura, I. , Inoue, M. , Shimoda, T. , Katori, K. , Nakayama, S., Physical Review C, 27, 2029-2036, 1983 "Copyright (1983) by the American Physical Society."
Note	

Osaka University Knowledge Archive : OUKA

<https://ir.library.osaka-u.ac.jp/repo/ouka/all/>

Correlations between the alpha particles and ejectiles in the 208 MeV ^{14}N on ^{93}Nb reaction at three different ejectile angles

T. Fukuda

Department of Physics, Osaka University, Toyonaka, Osaka 560, Japan

M. Ishihara

Institute of Physical and Chemical Research, Wako-Shi, Saitama 351, Japan

M. Tanaka

Kobe Tokiwa Junior College, Nagata, Kobe 653, Japan

H. Ogata, I. Miura, and M. Inoue

Research Center for Nuclear Physics, Osaka University, Ibaraki, Osaka 567, Japan

T. Shimoda and K. Katori

Laboratory of Nuclear Studies, Osaka University, Toyonaka, Osaka 560, Japan

S. Nakayama

College of General Education, Tokushima University, Tokushima 770, Japan

(Received 12 November 1982)

The in plane correlations between alpha particles and various ejectiles were investigated in the reaction of 208 MeV ^{14}N on ^{93}Nb at $\theta_{\text{HI}} = +22^\circ$, $+50^\circ$, and $+80^\circ$. There were three sources of coincident alpha particles: (i) the sequential alpha decay of the excited ejectiles, (ii) the equilibrium alpha emission from the targetlike fragments, and (iii) the nonequilibrium process. Process (i) contributed mainly to the cross sections with the angular range of θ_α close to θ_{HI} . Process (ii) contributed to the lowest part of the alpha energy spectra irrespectively of θ_{HI} and θ_α . The remaining part was ascribed to process (iii). For this process the differential coincidence cross section of the lower energy part of the alpha particles was approximately factorized as

$$d^4\sigma/d\Omega_{\text{HI}}d\Omega_\alpha dE_{\text{HI}}dE_\alpha = K (d^2\sigma/d\Omega_{\text{HI}}dE_{\text{HI}})_{\text{singles}} (d^2\sigma/d\Omega_\alpha dE_\alpha)_{\text{singles}}$$

with $K \sim 0.4/\text{b}$, whereas the higher energy part of the alpha particles emitted at the forward angles had a tendency to coincide weakly with the ejectiles emitted at the backward angles ($\theta_{\text{HI}} = +50^\circ$ and $+80^\circ$) as compared to the lower energy part of the alpha particles.

NUCLEAR REACTIONS $^{93}\text{Nb}(^{14}\text{N}, \text{HI}\alpha)$, $E=208$ MeV, $\theta_{\text{HI}}=22^\circ, 50^\circ, 80^\circ$; measured two-dimensional HI- α coincident energy and angular correlations; deduced reaction mechanisms.

I. INTRODUCTION

Particle-particle correlations¹⁻⁶ have attracted much current interest particularly in connection with the strong emission of "fast" light particles, which are widely observed in the light heavy-ion ($A \lesssim 20$) induced reactions and considered to contain important information about the heavy-ion reaction mechanisms. Recent measurements^{5,6} of alpha par-

ticle versus ejectile (HI) correlations have indicated that there exist at least three sources of coincident alpha particles: (i) the sequential alpha decay of the excited ejectiles, (ii) the equilibrium alpha emission from the targetlike fragments, and (iii) a nonequilibrium process of direct ternary nature. The former two processes are associated with a familiar mechanism, which occurs when the ejectiles and/or the targetlike fragments are excited above the particle-

emission threshold energy, whereas the last process appears to represent a particular aspect of heavy ion reactions involving emission of fast alpha particles.

The authors of Ref. 1 suggested that the non-

equilibrium process was characterized by an ability to factorize the coincidence cross section as a product of the singles cross sections, i.e.,

$$d^4\sigma/d\Omega_{\text{HI}}d\Omega_{\alpha}dE_{\text{HI}}dE_{\alpha}=K(d^2\sigma/d\Omega_{\text{HI}}dE_{\text{HI}})_{\text{singles}}(d^2\sigma/d\Omega_{\alpha}dE_{\alpha})_{\text{singles}}, \quad (1)$$

where K is a constant and found to be 0.3–0.5/b. This expression implies that the energy spectrum and angular distribution of each of the coincident fragments have shapes identical to those of the singles, when they are projected on the relevant coordinates. They claimed that this correspondence between the singles and coincidence results was an indication of a two-step mechanism in which the alpha particle was first emitted in the early stage of the reaction via a projectile fragmentationlike phenomenon, and the remaining fragment subsequently underwent deep inelastic scattering with the target in a manner “uncorrelated” with the first process.

Experimentally, the signature of Eq. (1) was reported to be observed in the reaction $^{58}\text{Ni} + ^{14}\text{N}$ at 148 MeV.¹ However, this feature was obscured in the reactions^{2,3} of $^{197}\text{Au} + ^{16}\text{O}$ at 310 MeV and $^{93}\text{Nb} + ^{16}\text{O}$ at 204 MeV because of the strong contribution from the sequential ejectile decay. Thus, in order to establish the properties of the nonequilibrium process, a measurement which enables separation from the sequential ejectile decay appears to be very important. In addition, the behavior of the nonequilibrium process over a wide angular range of ejectile and alpha particles should be studied to understand the overall features of the phenomena. The present study concerns these points; it consists of measurements of alpha-HI correlations in the reaction $^{93}\text{Nb} + ^{14}\text{N}$ at 208 MeV with three different angles, $\theta_{\text{HI}} = +22^\circ$, $+50^\circ$, and $+80^\circ$. This work is an extension and further elaboration on our previous investigation⁶ of alpha-HI correlations in the reaction $^{93}\text{Nb} + ^{14}\text{N}$ at 208 MeV with $\theta_{\text{HI}} = +22^\circ$. As discussed later, the alpha particles due to the sequential ejectile decay tend to appear in the angular range close to θ_{HI} , while those for the nonequilibrium process are found in the forward angular range independent of θ_{HI} . This fact facilitated the separation of two processes in the measurements for backward angles of θ_{HI} . As is also discussed later, the equilibrium alpha emission from the targetlike fragments was well separated from the nonequilibrium process in this experiment. Then we observed the following for the nonequilibrium process: (a) the differential coincidence cross section of the

lower energy part of the alpha particles was approximately factorized as Eq. (1) with $K \sim 0.4/b$, and (b) the higher energy part of the alpha particles emitted at the forward angles ($|\theta_{\alpha}| \lesssim 20^\circ$) had a tendency to coincide weakly with the ejectiles emitted at the backward angles ($\theta_{\text{HI}} = +50^\circ$ and $+80^\circ$) as compared to the lower energy part of the alpha particles. Thus, the coincidence cross section could not be simply factorized as Eq. (1).

In Sec. II the experimental procedures are described. The experimental results are presented in Sec. III. The discussions about the sequential ejectile decay, the equilibrium emission from the targetlike fragments, and the nonequilibrium process are presented in Secs. IV A–C, respectively.

II. EXPERIMENTAL PROCEDURES

The experiment was performed at the 230 cm AVF cyclotron of the Research Center for Nuclear Physics at Osaka University. A ^{93}Nb metallic foil of about 5 mg/cm² thickness was bombarded by a 208 MeV ^{14}N beam. Ejectiles (Li-C) were identified by a conventional 30 (or 15) μm ΔE and 5000 μm E Si telescope. The telescope was placed at three fixed angles of $\theta_{\text{HI}} = +22^\circ$, $+50^\circ$, and $+80^\circ$ and subtended solid angles of $\Omega = 3.6$, 10.3, and 31.4 msr, respectively. The low energy cutoff in the energy spectra caused by the ΔE detector was not significant even for the carbon isotopes at $\theta_{\text{HI}} = +80^\circ$. Four identical triplet telescopes, which consisted of 30 μm ΔE_1 , 300 μm ΔE_2 , and 5000 (or 3000) μm E Si detectors, were used to detect coincident alpha particles. These telescopes typically subtended solid angles of $\Omega = 2.0$ –9.0 msr. The angular correlations were measured for each ejectile angle θ_{HI} by placing the alpha detectors at angles θ_{α} between -50° and $+60^\circ$, and at a far backward angle of $\theta_{\alpha} = -135^\circ$ (or -160°) in the reaction plane, which is defined by the beam axis and the direction of the ejectile detector. A set of six signals consisting of $(\Delta E, E)$ of ejectiles, $(\Delta E_1, \Delta E_2, E)$ of alpha particles, and the time difference (time-to-amplitude converter) between two telescopes, was stored event by event on magnetic tape and was analyzed off line.

The amounts of carbon and oxygen contaminants

in the target were estimated to be less than 3 and 5 $\mu\text{g}/\text{cm}^2$ based on a measurement on the elastic scattering of 120 MeV alpha particles.

The coincidence cross section was measured for carbon and Mylar targets in order to evaluate the contributions from the carbon and oxygen contaminants. They were found to be less than 5% of the total coincidence events for most of the different coincidence settings and no correction was made. The absolute magnitude of the cross section was determined within 20%; the error bars in the figures are due to statistical errors.

III. EXPERIMENTAL RESULTS

A. Alpha-HI correlations at $\theta_{\text{HI}} = +22^\circ$

The details of the results for $\theta_{\text{HI}} = +22^\circ$ are given in Ref. 6. In short, they can be summarized as fol-

lows. Three processes contributed to the coincident alpha particles.

Process (i): The coincident events with θ_α close to θ_{HI} showed characteristic features of the sequential alpha-decay process of the excited ejectiles (see also Sec. IV A). It was found that the coincidence cross section of this process was approximately factorized by a product of the singles cross section

$$(d^2\sigma/d\Omega_{(\text{HI}+\alpha)}dE_{(\text{HI}+\alpha)})_{\text{singles}}$$

of the excited parent ejectiles (observed $\text{HI}+\alpha$) and the excitation energy spectrum $f(E_{\text{HI}-\alpha})$ of the parent ejectiles excited above the threshold of the alpha particle emission; i.e.,

$$d^4\sigma/d\Omega_{(\text{HI}+\alpha)}d\Omega_{(\text{HI}-\alpha)}dE_{(\text{HI}+\alpha)}dE_{(\text{HI}-\alpha)} = Nf(E_{\text{HI}-\alpha})(d^2\sigma/d\Omega_{(\text{HI}+\alpha)}dE_{(\text{HI}+\alpha)})_{\text{singles}} \quad (2)$$

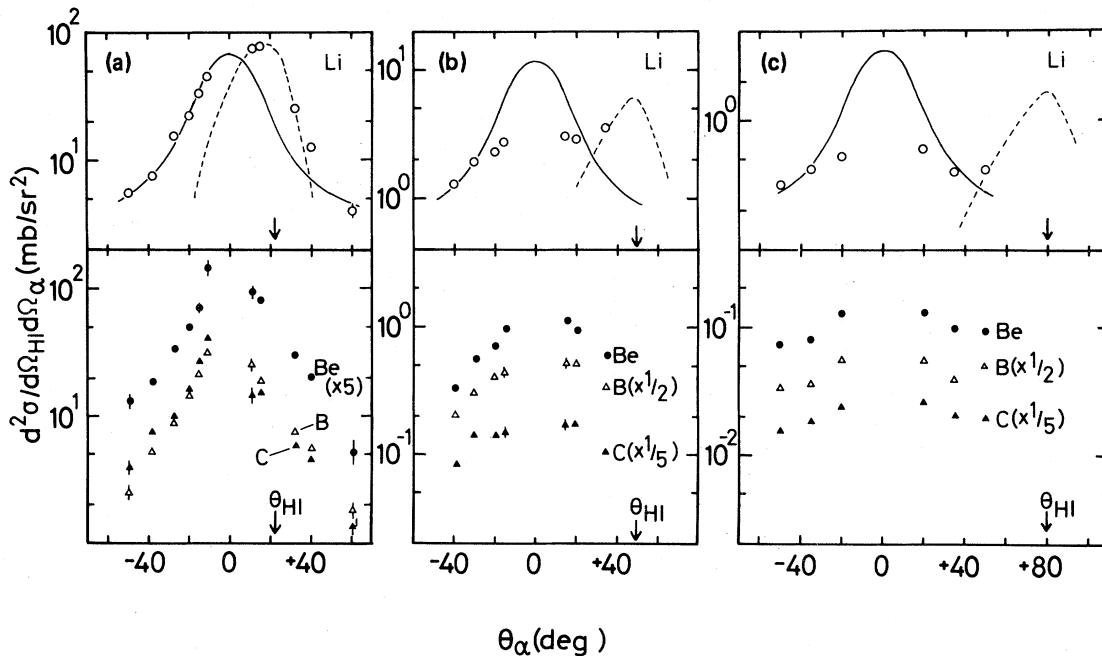


FIG. 1. The energy integrated angular distributions of the alpha particles coincident with various ejectiles as a function of the laboratory angle θ_α . (a)–(c) correspond to the ejectile angles $\theta_{\text{HI}} = +22^\circ$, $+50^\circ$, and $+80^\circ$, respectively. The solid lines represent the angular dependence of the singles cross section of the alpha particles. The dashed lines represent the calculated angular distributions of the sequential ejectile decay process for the $\alpha + \text{Li}$ channel based on the approximate formula (2) in Sec. III A. They are normalized to the data points at $\theta_\alpha = +15^\circ$, $+35^\circ$, and $+50^\circ$ for $\theta_{\text{HI}} = +22^\circ$, $+50^\circ$, and $+80^\circ$, respectively.

Here $E_{(HI+\alpha)}$ and $E_{HI-\alpha}$ are, respectively, the kinetic energy of the parent ejectile and the relative kinetic energy between the observed HI and alpha particle, $\Omega_{(HI+\alpha)}$ and $\Omega_{HI-\alpha}$ are the corresponding solid angles, and N is a normalization constant. By using Eq. (2) the angular distribution of the sequential ejectile decay process was calculated. The result for the $\alpha+{}^7\text{Li}$ channel, ${}^{11}\text{B}^* \rightarrow \alpha + {}^7\text{Li}$, is indicated by the dashed line together with the experimental data (open circle) in Fig. 1(a). As seen in the figure, this process primarily contributed to the angular range of θ_α confined close to the ejectile angle θ_{HI} . Further details of the calculation will be discussed in Sec. IV A.

Process (ii): The lowest part of the alpha energy spectra ($E_\alpha \lesssim 25$ MeV) was ascribed to the equilibrium emission from the targetlike fragments (see Sec.

IV B).

Process (iii): The remaining fraction of the cross section was ascribed to a nonequilibrium process. This process was predominant for the alpha particles detected on the opposite side ($\theta_\alpha < 0$) of the ejectile detector with respect to the beam direction, and in that angular range it showed behavior approximately following the factorization formula (1). This feature is shown in the Figs. 1(a) and 2(a) by comparing the coincidence yields with the singles (solid lines). The behavior of the nonequilibrium process in the angular range $\theta_\alpha > 0$ was obscured by the presence of the sequential ejectile decay. The detailed analysis in Ref. 6 suggests that the strength of the nonequilibrium process was somewhat smaller for $\theta_\alpha > 0$ than for $\theta_\alpha < 0$.

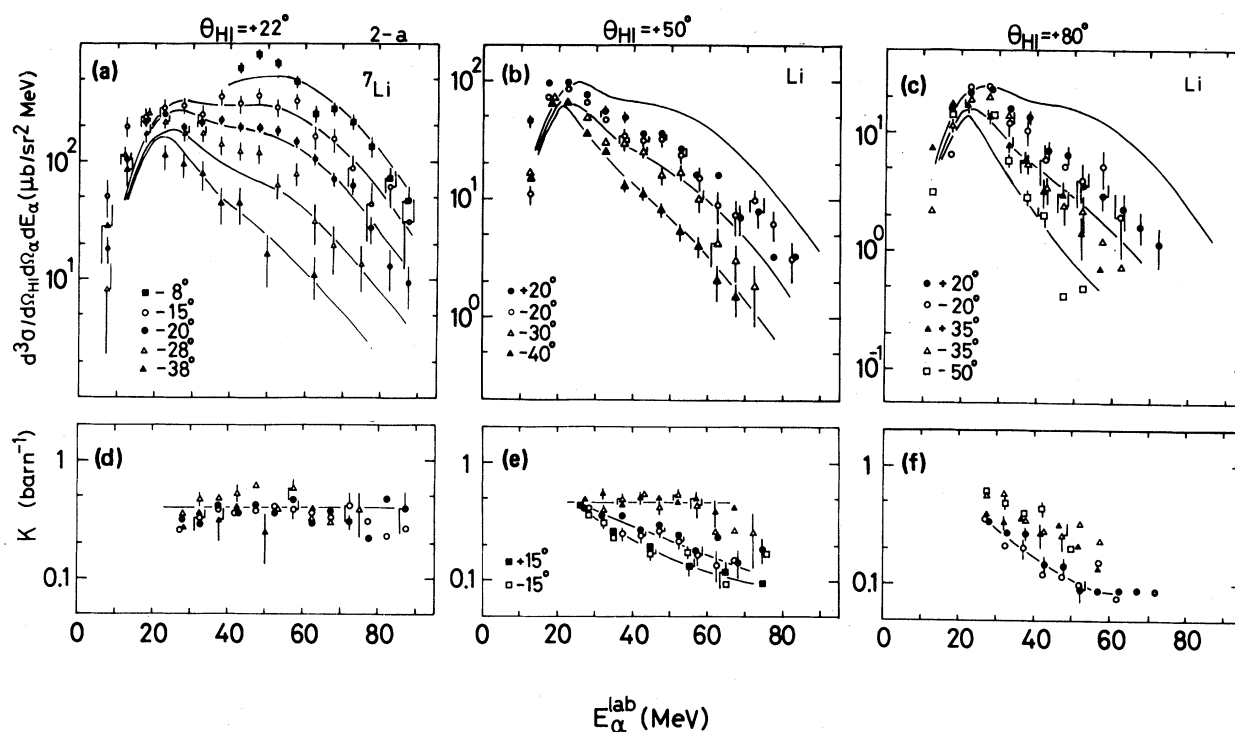


FIG. 2. The projected energy spectra of the alpha particles in coincidence with Li at $\theta_{HI} = +22^\circ$, $+50^\circ$, and $+80^\circ$, are depicted in (a)–(c), respectively. The angles indicated in figures are for alpha particles. The solid lines in (a)–(c) represent, respectively, the spectral shapes of the singles alpha particles for $\theta = 8^\circ, 15^\circ, 20^\circ, 28^\circ$, and 38° , $\theta = 20^\circ, 30^\circ$, and 40° , and $\theta = 2^\circ, 35^\circ$, and 50° in the descending order. In (d)–(f) the ratio K of the coincidence cross section to the product of the two singles ones, defined as $K = (d^4\sigma/d\Omega_{HI}d\Omega_\alpha dE_{HI}dE_\alpha) / ((d^2\sigma/d\Omega_{HI}dE_{HI})_{singles}(d^2\sigma/d\Omega_\alpha dE_\alpha)_{singles})$, are plotted as a function of the alpha energy E_α for the $\alpha + \text{Li}$ channel at $\theta_{HI} = +22^\circ, +50^\circ$, and $+80^\circ$, respectively. The symbols of the data in (d)–(f) represent the same angles θ_α indicated in (a)–(c), respectively. The data at angles of $\theta_\alpha = \pm 15^\circ$ are also depicted in (e). The solid lines in (d)–(f) are drawn only to guide the eye.

B. Alpha-HI correlations at $\theta_{\text{HI}} = +50^\circ$ and $+80^\circ$

The energy integrated angular distributions of the coincident alpha particles are shown in Figs. 1(b) and (c) for $\theta_{\text{HI}} = +50^\circ$ and $+80^\circ$, respectively. As discussed in Sec. IV A, the data with the angular range of θ_α close to θ_{HI} were affected by the strong contribution from the sequential ejectile decay process, while the results at the other angles could be considered to be essentially free from such a process. The angular distributions are almost symmetric with respect to the beam direction, except for the data at the θ_α nearest to θ_{HI} . It should be remarked that the slopes of the angular distributions are flat as compared to those of singles (solid lines). This feature is quite different from that for $\theta_{\text{HI}} = +22^\circ$.

Figures 2(b) and (c) show the projected energy spectra of the coincidence alpha particles with various θ_α for the $\alpha + \text{Li}$ channel. The shapes of the energy spectra for the other channels are almost the same as this case independently of the choice of the coincident ejectile. It is found that the energy spectra of the coincident alpha particles at θ_α have almost the same shapes as those at the symmetric angle $-\theta_\alpha$. These coincidence spectra at the backward angles ($|\theta_\alpha| > 20^\circ$) have shapes almost identical to those of the singles spectra (solid lines) taken at the same angles. On the other hand, the coincidence spectra at the forward angles ($\theta_\alpha = \pm 20^\circ$) show appreciable deviation from the corresponding singles spectra, being fairly reduced in the higher energy part of the spectrum. Therefore, the characteristics of the data are significantly different from those for $\theta_{\text{HI}} = +22^\circ$. Here, the agreement with the factorization prescription was deteriorated for the higher energy part of the alpha particles and the forward angles ($|\theta_\alpha| \lesssim 20^\circ$).

As shown in Fig. 3, the projected energy spectra of the coincident ejectiles for the $\alpha + \text{Li}$ channel turn out to have shapes similar to those of singles (solid lines) independently of θ_α . The same is true for the other ejectiles. It should be remarked that the singles energy spectra at $\theta_{\text{HI}} = +50^\circ$ and $+80^\circ$ primarily consist of the fully damped component.

IV. DISCUSSION

In the previous sections, we have noticed that there are at least three processes for the coincident alpha particle emission. In this section we discuss these processes in detail. In Secs. IV A and B, the sequential ejectile decay and the equilibrium evaporation from the targetlike fragments are discussed, respectively. In Sec. IV C the nonequilibrium process observed at three ejectile angles will be dis-

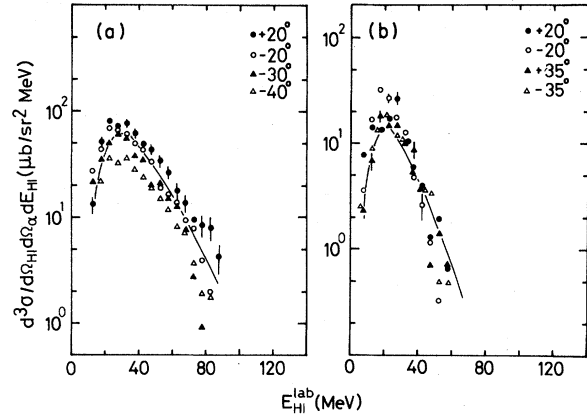


FIG. 3. The projected energy spectra of Li in coincidence with the alpha particles at the various angles θ_α for $\theta_{\text{HI}} = +50^\circ$ (a) and $+80^\circ$ (b). The solid lines in (a) and (b) represent the spectral shapes of the singles Li at $\theta = 50^\circ$ and 80° , respectively.

cussed. In this section we mainly discuss the $\alpha + \text{Li}$ channel because the characteristic features are the same for the other ejectiles.

A. The sequential ejectile decay process

As discussed in detail in Ref. 6, the coincidence events detected for the geometry with θ_α close to $\theta_{\text{HI}} = +22^\circ$ were characterized by the following features: (a) energy-energy correlations between the alpha particles and ejectiles showed two strong clusters, which corresponded to forward and backward emission of the alpha particles with respect to the direction of the motion of the excited parent ejectiles; (b) the $E_{\text{HI}-\alpha}$ spectra deduced by using three body kinematic relations⁷ showed peaks of fine structure which may be ascribed to the alpha decay of isolated excited states of the $(\text{HI} + \alpha)$ nucleus.

Therefore, the coincidence events with θ_α close to $\theta_{\text{HI}} = +22^\circ$ were ascribed to the sequential ejectile decay process. For this process it was found that the coincidence cross section was approximately factorized as Eq. (2) in Sec. III A. By using Eq. (2) the angular distribution of the sequential ejectile decay process was calculated for the $\alpha + {}^7\text{Li}$ channel as shown in Fig. 1(a) by a dashed line. In the calculation the $E_{\text{HI}-\alpha}$ spectrum obtained in the coincidence measurement with $\theta_\alpha = +32^\circ$ and $\theta_{\text{HI}} = +22^\circ$ and the inclusive differential cross section of ${}^{11}\text{B}$ obtained from a separate measurement⁸ were, respectively, used for $f(E_{\text{HI}-\alpha})$ and

$$(d^2\sigma/d\Omega_{(\text{HI}+\alpha)}dE_{(\text{HI}+\alpha)})_{\text{singles}}$$

in Eq. (2).

Assuming the same Eq. (2) with the same $E_{\text{HI}-\alpha}$ spectra as $\theta_{\text{HI}} = +22^\circ$, and the inclusive cross section of Boron in Ref. 8, we calculated the sequential decay process at $\theta_{\text{HI}} = +50^\circ$ and $+80^\circ$. The results are shown by dashed lines in Figs. 1(b) and (c) for $\theta_{\text{HI}} = +50^\circ$ and $+80^\circ$, respectively. They are found to contribute to the cross section with the confined angular range of θ_α close to the ejectile angle θ_{HI} . The calculated cross sections were normalized to the data points at $\theta_\alpha = +35^\circ$ and $+50^\circ$, respectively, where the data showed the characteristic features (a) and (b). As shown in Figs. 1(b) and (c), even if the ejectile sequential decay process is totally responsible for the coincidence cross section at the angles of $\theta_\alpha = +35^\circ$ and $+50^\circ$ for $\theta_{\text{HI}} = +50^\circ$ and $+80^\circ$, respectively, the data at the other angles can be considered to be essentially free from such a process. This point should be stressed because the α -HI coincidence data now available in the light heavy ion reactions¹⁻⁶ suffer from the strong disturbance of the sequential ejectile decay over the wide angular range observed and careful analyses were made in order to extract reliable information on the nonequilibrium process.

B. The equilibrium evaporation from the targetlike fragments

To evaluate the contribution of the equilibrium alpha emission from the targetlike fragments, we transformed the laboratory alpha energy spectra $d^3\sigma/d\Omega_{\text{HI}}d\Omega_\alpha dE_\alpha$ at various angles, including the far backward angle, into the moving frame of the targetlike fragments by using the three body kinematic relations.⁷ In this transformation the Jacobian between the two coordinate systems was properly taken into account. It should be noted that this procedure is equivalent to that of estimating the cross section in the moving frame by using the invariant cross section $d^3\sigma/dv^3$. The resulting energy spectra at various θ_α with $\theta_{\text{HI}} = +80^\circ$ are given in Fig. 4 together with that of the far backward angle of $\theta_\alpha = -135^\circ$, where the equilibrium emission from the targetlike fragments only may be available. We find that the lowest parts of the energy spectra of various θ_α are almost identical to that of $\theta_\alpha = -135^\circ$, whereas the cross section of various θ_α for $E_\alpha \geq 20-25$ MeV (roughly corresponding to 27-32 MeV in the laboratory energy) are much larger than that of $\theta_\alpha = -135^\circ$. The lowest parts of the energy spectra of the coincident alpha particles show the almost isotropic distribution in the moving frame of the targetlike fragment and are considered to be due to the equilibrium emission from the targetlike fragments, whereas the coincident fast alpha

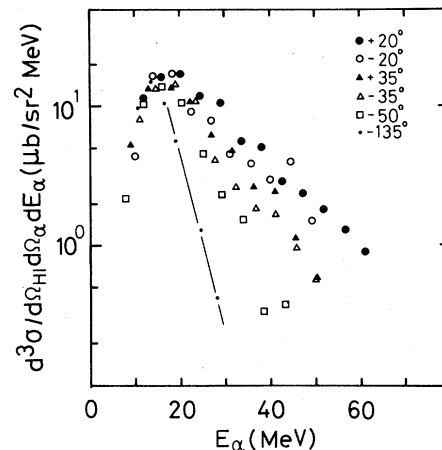


FIG. 4. The energy spectra of the alpha particles in coincidence with Li at $\theta_{\text{HI}} = +80^\circ$ in the moving frame of the targetlike fragments. The solid line is drawn using the form of $\exp(-E_\alpha/T)$ with $T = 3$ MeV.

particles ($E_\alpha \geq 25$ MeV) are mainly attributed to a nonequilibrium process. A similar conclusion was drawn for $\theta_{\text{HI}} = +22^\circ$ and $+50^\circ$. The equilibrium emission was found to be less significant as θ_{HI} decreased because the inelasticity of the reaction decreased.

C. The nonequilibrium process of the coincident alpha particles

The remaining part of the coincident events other than (i) the sequential ejectile decay process and (ii) the equilibrium evaporation from the targetlike fragments, was, most likely, ascribed to the nonequilibrium process. Process (i) significantly affected the data of $\theta_\alpha > 0$, $\theta_\alpha = +35^\circ$ and $+50^\circ$ for $\theta_{\text{HI}} = +22^\circ$, $+50^\circ$, and $+80^\circ$, respectively, and process (ii) dominated the data for $E_\alpha \leq 25$ MeV, irrespective of θ_{HI} and θ_α . Therefore, in order to make the discussion of the nonequilibrium process clear, we primarily confined ourselves to data other than these.

To see the overall feature of the nonequilibrium process, the coincidence cross section was compared with the singles ones of α and HI; the factor K of Eq. (1) in Sec. I was deduced as a function of θ_{HI} , θ_α , and E_α . The dependence of K on E_{HI} was neglected because the projected energy spectra of the coincidence ejectiles had shapes similar to those of singles (see Fig. 3).

In Figs. 2(d)–(f) the values of K are plotted as a function of E_α for various cases of θ_{HI} and θ_α . In the lower energy part of the alpha particles, K has an approximately constant value of about $0.4/b$ ir-

respective of θ_{HI} , and the approximate symmetry about the beam axis appears more or less to hold. These features are similar to those discussed in Ref. 1 for the coincident alpha particles (note that a value of $0.3-0.5/b$ was obtained in Ref. 1).

On the other hand, an outstanding deviation from the constant value is observed in the higher energy part of the alpha particles emitted at the forward angles ($|\theta_\alpha| \lesssim 20^\circ$). In the case of $\theta_{HI} = +22^\circ$, K is approximately constant even for the higher energy part of the alpha particles, independent of θ_α . However, the deviation is evident for the cases of $\theta_{HI} = +50^\circ$ and $+80^\circ$. The deviation is more pronounced for more backward θ_{HI} and more forward θ_α , where K decreases to $0.1/b$.

The observed results are in contrast with the observation of Ref. 1 that nonequilibrium alpha-particle emissions universally have the property of "uncorrelated" nature characterized by the constant K value for the coincidence cross sections. While this is the case for the lower energy part of the alpha particles, the higher energy part shows the property of "correlated" nature in the sense that the forward emitted alpha particles coincide more (less) favorably with the forward (backward) emitted ejectiles. This observation indicates that different reaction mechanisms may be dominant for the lower- and higher-energy parts, and thus modification for the argument of Ref. 1 is needed.

The authors of Ref. 1 inferred that the nonequilibrium emission process may proceed in two steps where the alpha particle was emitted at an early stage of the reaction in the fragmentationlike process of the projectile, and the rest of the projectile subsequently underwent deep inelastic scattering with the target. However, it is not obvious that such a two step reaction will necessarily lead to the factorization formula of Eq. (1). For the relatively simple process supposed it is rather probable that the alpha particle and ejectile memorize the initial correlation in the projectile even after the strong interaction with the target nucleus at the second stage of the reaction is imposed. In that case an emission of correlated nature may arise, showing a tendency that the alpha particles be emitted in a narrow cone on the opposite side of the ejectile with respect to the beam direction. Moreover, such alpha particles may tend to have energies corresponding to the beam velocity, since the simple fragmentation process is assumed. These features appear to be consistent with the observed properties of the higher energy part of the coincident alpha particles.

On the other hand, the uncorrelated emission is dominant for alpha particles with lower energies, indicating that the alpha particles are emitted via a

complicated multistep reaction rather than in a simple projectile fragmentationlike process, as is conceived for the higher energy part. For instance, one may even conceive a process in which the alpha particles cannot be well defined as originating from the projectile or target. In such a case the angular distribution of the alpha particles is likely to be less influenced by the direction of the projectile or ejectile; this is indeed observed for the lower energy part of the coincident alpha particles.

The coexistence of two components in the nonequilibrium alpha emission suggested by the present coincidence data was also indicated by the inclusive measurements of the alpha particles in the same reaction system $^{93}\text{Nb} + ^{14}\text{N}$ at 132, 159, and 208 MeV (Ref. 9) and in the Ni, Ag, and Ta + 860 MeV ^{20}Ne reaction.¹⁰ These experiments showed that extra enhancement of the cross section is significant in the energy region comparable to the beam velocity, which appears on top of the more generally observed component with an exponentiallike energy spectrum and a smaller mean energy. Such an extra enhancement is observed to be more significant at more forward angles and to increase with incident energy. It appears, in view of corresponding energies, that the component associated with the extra enhancement in the inclusive measurements is relevant to the coincident alpha particles with higher energies, while the other component with an exponentiallike energy spectrum is relevant to those with lower energies.

To summarize, we have mainly studied the nonequilibrium process of alpha particles in the coincidence measurement with ejectiles. The nonequilibrium process is distinguished from the alpha emission associated with sequential evaporation from the products of the primary binary reaction. The analysis on energy and angular dependence of the K value indicates that there exist at least two different components of nonequilibrium alpha emission: one is dominant in the higher energy part comparable to the beam velocity, and the other in the lower energy part. While this observation appears to be in accord with recent results of inclusive alpha particle spectra, we note that no indication of the two components was reported in Ref. 1, where a similar study of alpha-ejectile correlation was made for the $^{58}\text{Ni} + ^{14}\text{N}$ reaction at 148 MeV. This difference between the two reactions may be attributed mainly to the different incident energies (210 MeV vs 148 MeV), since the inclusive data indicate that occurrence of the component associated with the beam velocity becomes increasingly important as the incident energy is increased. Further study of this subject, particularly concerning the incident energy dependence, appears to be important.

ACKNOWLEDGMENTS

We gratefully acknowledge the cyclotron crew for their assistance. This experiment was performed at

the Research Center for Nuclear Physics, Osaka University, under Program Nos. 10A-17 and 11A-19.

-
- ¹R. K. Bhowmik, E. C. Pollacco, N. E. Sanderson, J.B.A. England, and G. C. Morrison, *Phys. Rev. Lett.* **43**, 619 (1979).
- ²M. Bini, C. K. Gelbke, D. K. Scott, T. J. M. Symons, P. Doll, D. L. Hendrie, J. L. Laville, J. Mahoney, M. C. Mermaz, C. Olmer, K. Van Bibber, and H. H. Wieman, *Phys. Rev. C* **22**, 1945 (1980).
- ³G. R. Young, R. L. Ferguson, A. Gavron, D. C. Hensley, Felix E. Obenshain, F. Plasil, A. H. Snell, M. P. Webb, C. F. Maguire, and G. A. Petitt, *Phys. Rev. Lett.* **45**, 1389 (1980).
- ⁴H. Ho, P. Gonthier, M. N. Namboodiri, J. B. Natowitz, L. Adler, S. Simon, K. Hagel, R. Terry, and A. Khodai, *Phys. Lett.* **96B**, 51 (1980).
- ⁵J. van Driel, S. Gonggrijp, R. V. F. Janssens, R. H. Siemssen, K. Siwek-Wilczynska, and J. Wilczynski, *Phys. Lett.* **98B**, 351 (1981).
- ⁶T. Fukuda, M. Ishihara, M. Tanaka, I. Miura, H. Ogata, and H. Kamitsubo, *Phys. Rev. C* **25**, 2464 (1982).
- ⁷G. G. Ohlsen, *Nucl. Instrum. Methods* **37**, 240 (1965).
- ⁸T. Fukuda, M. Tanaka, M. Ishihara, H. Ogata, I. Miura, and H. Kamitsubo, *Phys. Lett.* **99B**, 317 (1981).
- ⁹T. Fukuda, M. Ishihara, H. Ogata, I. Miura, T. Shimoda, K. Katori, S. Shimoura, M.-K. Tanaka, and E. Tanaka (unpublished).
- ¹⁰J. B. Natowitz, M. N. Namboodiri, L. Adler, R. P. Schmitt, R. L. Watson, S. Simon, M. Berlinger, and R. Choudhury, *Phys. Rev. Lett.* **47**, 1114 (1981).